INORGANIC CHEMISTRY

FRONTIERS

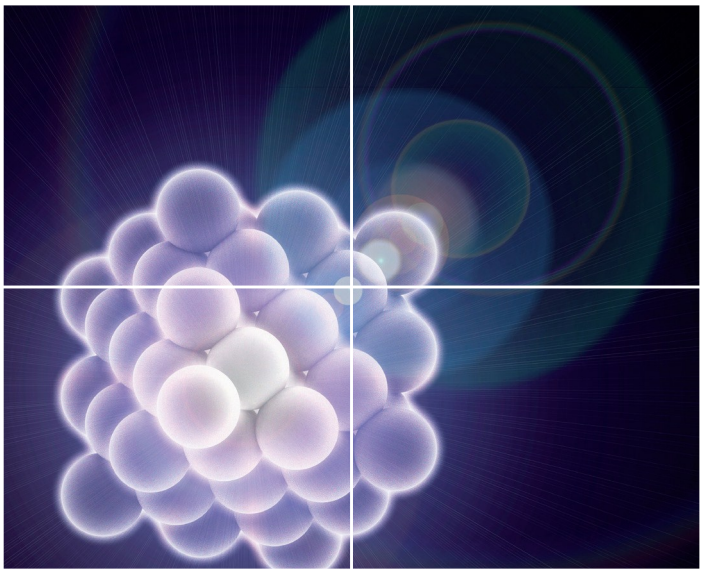

Accepted Manuscript

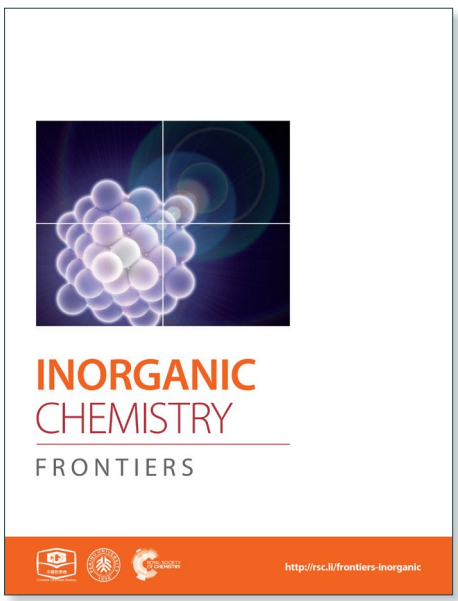

This is an *Accepted Manuscript*, which has been through the Royal Society of Chemistry peer review process and has been accepted for publication.

Accepted Manuscripts are published online shortly after acceptance, before technical editing, formatting and proof reading. Using this free service, authors can make their results available to the community, in citable form, before we publish the edited article. We will replace this *Accepted Manuscript* with the edited and formatted *Advance Article* as soon as it is available.

You can find more information about *Accepted Manuscripts* in the **Information for Authors**.

Please note that technical editing may introduce minor changes to the text and/or graphics, which may alter content. The journal's standard **Terms & Conditions** and the **Ethical guidelines** still apply. In no event shall the Royal Society of Chemistry be held responsible for any errors or omissions in this *Accepted Manuscript* or any consequences arising from the use of any information it contains.

Journal Name

ARTICLE

Magnetization Dynamics of a Heterometallic Dy-isocarbonyl Complex

Received 00th January 20xx,
Accepted 00th January 20xx

DOI: 10.1039/x0xx00000x

www.rsc.org/

Courtney M. Dickie and Michael Nippe*

The reaction of $Dy(N(Si(CH_3)_3)_2)_3$ with three equivalents of $HW(CO)_3Cp$ (Cp = cyclopentadienyl) furnished the first structurally characterized isocarbonyl complex of Dy^{3+}, $[\{CpW(CO)_2(\mu\text{-}CO)\}_3Dy(thf)_5]$ (**1**). Solid dilution via cocrystallization with the isostrucutral Y^{3+} analogue of **1** allowed for the observation of temperature dependent signals in the out-of-phase component of the ac magnetic susceptibiilty in the presence of an applied dc field. An effective barrier to magnetization reversal of 12.6 cm^{-1} could be extracted for compound **1** under these conditions.

Introduction

Paramagnetic molecules that exhibit bistable high spin ground states and magnetic anisotropy can display energy barriers to reorientation of their molecular spins which can lead to slow magnetic relaxation dynamics and magnetic hysteresis.[1] Such molecules are commonly referred to as single-molecule magnets or SMMs and are being investigated for their potential applications for high density data storage. Since the discovery of slow magnetic relaxation in multinuclear transition metal complexes[2] research has focused on the development of mono-[3] and multi-nuclear[4] transition metal complexes. The large single ion anisotropy of lanthanide ions renders them attractive candidates in this regard and has led to the development of single-ion magnets with improved barriers to spin reorientation (U_{eff}).[5] The first lanthanide-based SMMs were lanthanide phthalocyanine sandwich complexes $[LnPc_2]^-$ (Ln = Tb, Dy) and a high U_{eff} of 230 cm^{-1} (331 K) was reported for diluted samples $[Bu_4N][Tb_{0.2}Y_{0.8}Pc_2]$.[6] A heteroleptic neutral $[Tb^{3+}(Pc)(Pc')]$ complex (Pc' = octa(tertbutylphenoxy)-substituted Pc ring) was shown to have an even higher U_{eff} of 652 cm^{-1} (938 K), currently a record in the field.[7] Diluted yttrium-doped polymetallic Dy and Tb poly-lanthanide alkoxide cage complexes, $Ln@\{Y_4K_2\}$, were found to have U_{eff} exceeding 556 cm^{-1} (800 K).[8] Notably, the blocking of relaxation via the first excited state led to these complexes possessing the second highest relaxation barriers reported and the slow magnetic relaxation was found to be single-ion in origin.

However, the plethora of lanthanide based SMMs suffer from quantum tunnelling of the magnetization (QTM) and modern approaches circumvent this by utilizing strong exchange coupling between lanthanide ions through radical bridges.[9] Magnetic coupling of lanthanide ions to transition metal ions has also been widely utilized in order to combine magnetic anisotropy and high spin states of lanthanide and transition metal ions. Most of these 4f-3d complexes feature bridging oxygen based ligands.[10] These studies are further complicated as subtle changes in the ligand field of the lanthanide ion influences the energies of low lying m_J states, thereby determining U_{eff}.[5c,11]

We have started a research program that aims at the discovery of new heterometallic lanthanide-transition metal complexes and their magnetic characterization. As part of this effort we utilize anionic metal-carbonyl fragments as ligands for lanthanide ions. These efforts are motivated by the degree of tunability of ligand field strength imposed by metal-carbonyl anions as a function of the nature of the transition metal employed.[12] Furthermore, utilization of paramagnetic metal carbonyl anions[13] as ligands would allow to study exchange coupling through carbonyl bridges.[14] Additionally, Ln-isocarbonyl complexes are potential precursors to lanthanide-transition metal bonds via photolysis: Recently, Arnold and co-workers demonstrated the formation of an uranium-cobalt bond via photolytic CO elimination of an U-isocarbonyl compound.[15]

We chose to start our investigations by characterizing the magnetic properties of a Dy-isocarbonyl complex, since Dy^{3+} is a highly anisotropic Kramers ion and its ground state is bistable, independent of ligand field.

Herein, we report the synthesis of $[\{CpW(CO)_2(\mu\text{-}CO)\}_3Dy(thf)_5]$ **1** via amine elimination reactions between $[Dy(N(SiMe_3)_2)_3]$ and $[HW(CO)_3Cp]$. Notably, this is the first report of a structurally characterized isocarbonyl complex of Dy.[16] Temperature dependent slow magnetic relaxation could be observed in dilute samples of **1·thf** (Y:Dy 12:1), with a barrier height (U_{eff}) of 12.6 cm^{-1} (18.1 K) under a 400 Oe applied dc field.

Experimental section

General considerations

[a] Department of Chemistry, Texas A&M University, 3255 TAMU, College Station, TX, 77843 (USA). E-mail: nippe@chem.tamu.edu

Electronic Supplementary Information (ESI) available: Structure tables, unit cell packing diagram, and additional magnetic data. See DOI: 10.1039/x0xx00000x

Unless otherwise noted, all reactions and manipulations were carried out under anaerobic and anhydrous conditions in an argon-filled glovebox (Vigor). Tetrahydrofuran (thf) and toluene were dried and deoxygenated using a solvent purification system (JC Meyer Solvent System) and stored over molecular sieves in an argon-filled glovebox. $[Dy(N(SiMe_3)_2)_3]$ and $[Y(N(SiMe_3)_2)_3]$ were prepared as previously described[17] and recrystallized from toluene. $HW(CO)_3Cp$ was purchased from Sigma-Aldrich and used as received. Elemental analyses were carried out by ALS Environmental (Tucson, AZ). IR spectra were recorded on a Mattson ATI Genesis FT-IR spectrometer fitted with a PIKE Technologies MIRacle ATR sampling accessory.

Synthesis of $[(thf)_5Dy((OC)W(CO)_2Cp)_3]$·thf (1·thf)

A solution of $HW(CO)_3Cp$ (63.0 mg, 0.185 mmol) in thf (3 mL) was added to a stirring solution of $Dy(N(SiMe_3)_2)_3$ (39.0 mg 0.0606 mmol) in thf (3 mL) and the reaction mixture was stirred for 1.5 h at rt. The solution was filtered through Celite and concentrated *in vacuo*. Very air-sensitive, yellow block-shaped crystals of **1·thf** (41.7 mg, 43 %) were obtained from the concentrated thf solution after 24 h at -30 °C. Anal. calcd for $C_{42}H_{51}DyW_3O_{13.5}$ (**1**-0.5thf): C, 33.95; H, 3.46. Found: C, 33.45; H, 3.49. IR: ν_{max} cm^{-1} = 2010s, 1894s, 1790br, 1680br, 1602br [all ν(CO)].

Modified Synthesis of $[(thf)_5Y((OC)W(CO)_2Cp)_3]$·thf (2·thf)

Prepared analogously to $[(thf)_5Dy((OC)W(CO)_2)_3]$. Yellow block-shaped crystals of **2·thf** were formed from a concentrated thf solution after 24 h at -30 °C. Yield: 64 %. Product was confirmed by comparing unit cell parameters to those of the previously reported structure.[18]

Synthesis of $[(thf)_5Dy_{0.08}Y_{0.92}((OC)W(CO)_2Cp)_3]$·thf

A solution of **1·thf** (7.28 mg, 0.0457 mmol) in thf (3 mL) and a solution **2·thf** (83.2 mg, 0.129 mmol) in thf (10 mL) were mixed. Yellow block-shaped crystals were obtained after 48 h at -30 °C. Yield: 77 %. Unit cell parameters (110 K): a = 11.21 Å, b = 11.32 Å, c = 20.83 Å, α = 97.4°, β = 101.2°, γ = 92.8°, V = 2562 Å^3.

X-ray crystallography

Single crystal X-ray diffraction measurements were carried out using a Bruker-AXS APEX-II CCD area detector diffractometer (Mo Kα radiation, λ = 0.71069 Å) diffractometer (NSF-CHE-9807975, NSF-CHE-0079822 and NSF-CHE-0215838). Crystals were mounted on nylon loops and cooled in a nitrogen stream (110(2) K). Bruker AXS APEX II software was used for data collection and reduction.[19] Absorption corrections were applied using SADABS.[20] Space group assignments were determined by examination of systematic absences, E-statistics, and successive refinement of the structures. Structures were solved using direct methods and refined by least-squares refinement on F2 followed by difference Fourier synthesis.[21] All hydrogen atoms were included in the final structure factor calculation at idealized positions and were allowed to ride on the neighbouring atoms with relative isotropic displacement coefficients. Thermal parameters were refined anisotropically for most non-hydrogen atoms. There is partial disorder of some of the carbon atoms of one of the Cp ligands. Crystallographic data for **1·thf** is given in Table S1. The structure of isostructural Y^{3+} analogue **2** was confirmed by unit cell determination to match the previously reported unit cell.[18]

Magnetic Measurements

Magnetic samples were prepared by adding crushed crystalline sample to a high-purity 7 mm NMR tube and covering it with a layer of eicosane. The NMR tube was flame sealed under vacuum and the eicosane was melted in a water bath at 35 °C, evenly dispersing it throughout the sample. The sample was loaded into a straw affixed to the end of the sample rod. Magnetic measurements were carried out using a Quantum Design MPMS XL SQUID magnetometer (NSF-9974899) (compound **1·thf**) and a Quantum Design MPMS 3 SQUID magnetometer (TAMU Vice President of Research) (dilution sample). Dc measurements were carried out over a temperature range of 1.8 to 300 K and an applied field of 1000 Oe. Ac measurements were carried out over a temperature range of 1.8 to 8 K, using a 2 to 5 Oe alternating field and applied dc fields of 0 to 2000 Oe. Data was corrected for sample holder and diamagnetic corrections were applied to the dc magnetic data of **1·thf**, accounting for contributions from eicosane and the core diamagnetism with the diamagnetic contribution from the complex estimated from Pascal's constants.[22] Cole-Cole plots (χ_M' vs χ_M'') were fitted using least-squares regression to formulae describing χ' and χ'' in terms of the variables constant temperature susceptibility (χ_T), adiabatic susceptibility (χ_S), relaxation time (τ) and the distribution of relaxation times (α).

Results and Discussion

Synthesis

The preparation of molecular and polymeric lanthanide isocarbonyl species has previously been reported via salt elimination reactions between lanthanide halide complexes and alkali metal salts of anionic transition metal carbonyl complexes. However, structural information for the early examples is not available.[23] More recently, molecular structures of lanthanide isocarbonyl complexes have been reported and it could be shown that alkane elimination reactions between lanthanide-alkyl complexes and transition metal hydrides are viable alternative synthetic routes.[18] Interestingly, we find that $HW(CO)_3Cp$ is sufficiently acidic to react smoothly with $[Dy(N(SiMe_3)_2)_3]$ in thf to form $[\{CpW(CO)_2(\mu\text{-}CO)\}_3Dy(thf)_5]$ **1** via an amine elimination reaction (Scheme 1). Large block-shaped crystals of **1·thf** are obtained from concentrated thf solutions at -30 °C over 24 h. Attempts to carry out the reaction and crystallizations in non-coordinating solvents were unsuccessful due to the limited solubility of $HW(CO)_3Cp$. The isostructural yttrium analogue **2·thf** has been reported previously prepared via alkane elimination. We found that **2·thf** can also be conveniently prepared from $[Y(N(SiMe_3)_2)_3]$ instead.

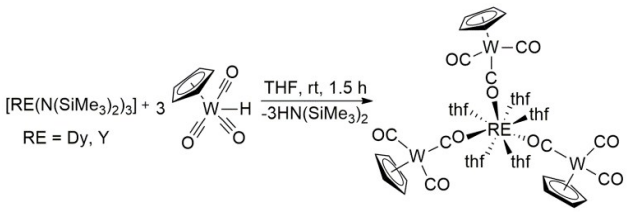

Scheme 1. Synthesis of $[\{CpW(CO)_2(\mu\text{-}CO)\}_3RE(thf)_5]$, RE = Dy (**1**) and Y (**2**).

Crystal Structure

Compound **1·thf** crystallizes in the triclinic space group $P\bar{1}$ (Table S1). X-ray diffraction studies revealed a distorted square antiprismatic geometry around the central Dy^{3+} ion. Three $[CpW(CO)_3]^-$ ligand moieties are coordinated to the Dy^{3+} centre through the carbonyl oxygen (d(Dy-O) = 2.320(5) Å, 2.270(5) Å, 2.267(5) Å) and five thf ligands (d(Dy-O_{thf}) = 2.384(5) – 2.462(5) Å) fill the rest of the coordination sphere (Figure 1, Table S2). The O-Dy-O angles concerning O donors of the same distorted square are in the range of 72°-75°. There is one additional non-coordinated thf molecule per molecule of **1** in the crystal lattice. Intermolecular $Dy^{3+}\cdots Dy^{3+}$ distances in crystals of **1·thf** are in the range of 10.45 to 13.66 Å, with the shortest interaction depicted in the unit cell packing diagram in Figure S1. Notably, this is the first structurally characterized example of a dysprosium isocarbonyl compound.

The W-C bond lengths to the bridging isocarbonyl moieties are with 1.875(8) - 1.894(8) Å shorter than those to the terminal carbonyl W-C bonds (1.939(7) - 1.955(8) Å). The C-O bond lengths of the bridging isocarbonyl groups are with 1.21(1) - 1.22(1) Å longer than those of the terminal carbonyl ligands (1.16(1) - 1.18(1) Å). The W-C-O (bridging) bond angles are nearly linear, with values of 177.4(7)°, 177.7(7)° and 177.9(6)°. The W-C (bridging) and C-O (bridging) bond distances and angles are in agreement with those observed in a tungsten isocarbonyl complex of cerium, $[Cp''_2Ce(\mu\text{-}OC)W(CO)(Cp)(\mu\text{-}CO)]_2$,[16q] and of yttrium, $[\{CpW(CO)_2(\mu\text{-}CO)\}_3Y(thf)_5]$.[18] We note that similar shortening and elongation of M-C and C-O distances, respectively, has also been well established for simple contact ion pairs of alkali metal salts of transition metal carbonyl anions; the presence of the cationic charge is hereby expected to lower LUMO energies of the respective CO ligand and results in increased π-backbonding from the transition metal.[24]

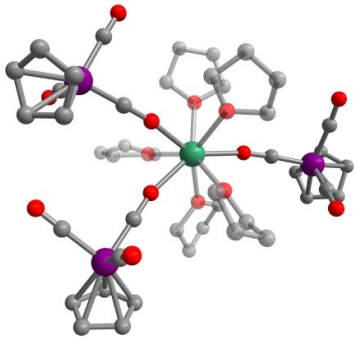

Figure 1. Molecular structure of **1** in **1·thf**. Green = Dy, purple = W, red = O, grey = C. Hydrogen atoms omitted for clarity.

Compound **1·thf** is isostructural to the yttrium analogue **2·thf** first prepared by Kempe *et al*. through an alkane elimination reaction between $[Y(CH_2SiMe_3)_3(thf)_2]$ and 3 equivalents of $[HW(CO)_3Cp]$.[18]

Magnetic Studies

Dc magnetic susceptibility data were collected for **1·thf** over the temperature range of 2 to 300 K under an applied field of 1000 Oe (Figure 2). The room temperature $\chi_M T$ value of 14.22 emu·K/mol is in agreement with the expected value (14.17 emu·K/mol) for a single Dy^{3+} ion ($^6H_{15/2}$, S=5/2, L=5, g=4/3). Upon cooling, a gradual decrease of $\chi_M T$ at around 100 K and a more rapid decrease below 50 K is observed, reaching a minimum value of 10.51 emu·K/mol at 2 K. This decrease at low temperature is attributed to thermal depopulation of the Stark sublevels of Dy^{3+} and possible antiferromagnetic dipole-dipole interactions between Dy^{3+} centres.[25]

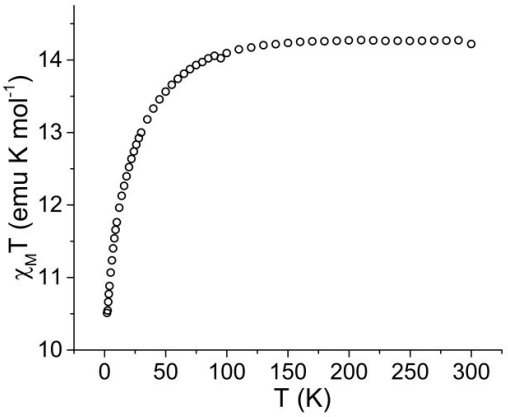

Figure 2. Temperature dependence of the molar magnetic susceptibility times temperature ($\chi_M T$) product for **1·thf** under a 1000 Oe applied dc field at temperatures 2 to 300 K.

To investigate magnetization dynamics of **1**, variable frequency ac susceptibility measurements were carried out on **1·thf**. In the absence of an applied dc field, no signal was observed in the out-of-phase (χ_M'') component of the ac magnetic susceptibility at frequencies up to 1000 Hz (Figure S2). The absence of a signal in χ_M'' under zero dc field could be due to quantum tunnelling, as this phenomenon is frequently observed in lanthanide-based SMMs.[26] One commonly used method to suppress quantum tunnelling is the application of a small dc field which lifts the degeneracy of energy levels, thereby preventing this relaxation path.[25,27] Application of a dc field of 1000 or 2000 Oe revealed a signal in the χ_M'' component. However the maxima of these signals lie outside the accessible frequency range of the instrument (1000 Hz) (Figure S2).

A common cause of quantum tunnelling in SMMs is intermolecular dipole-dipole interactions between paramagnetic metal centres, allowing for mixing of the ground states.[28] Dilution of a paramagnetic compound with an isostructural diamagnetic compound by co-crystallization is frequently carried out to suppress dipole-dipole interactions in Ln-SMMs.[5e,6] To probe the effect of Dy^{3+} dipole-dipole interactions on quantum tunnelling in **1·thf**, a solid magnetic dilution sample was prepared. The isostructural diamagnetic

Y^{3+} compound, **2·thf**, was prepared and crystals of a 12:1 dilution of Y:Dy were isolated.

Ac studies of the dilution sample under zero applied dc field between 1.8 and 4 K revealed a signal in the χ_M" component. However the maxima lie outside of the frequency range of the instrument (Figure 3). Application of variable strength dc fields at 1.8 K revealed slow relaxation of the magnetization, an increase in χ_M" and a shift in the maxima of χ_M" to lower frequencies (Figure S3). The largest signal in the out-of-phase component (χ_M") was obtained by applying a 400 Oe dc field. As a result, the remainder of the ac studies were carried out under a 400 Oe dc field.

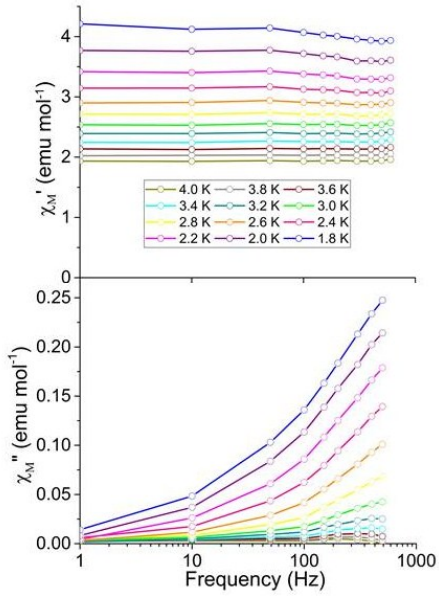

Figure 3. Frequency dependence of the in-phase (χ_M') (top) and out-of-phase (χ_M") (bottom) ac susceptibility measurements of a 12:1 (Y:Dy) magnetic dilution of **1·thf** under zero applied dc field and a 5 Oe switching field. Lines are a guide for the eye.

The temperature dependence of χ_M' and χ_M" were investigated under an applied dc field of 400 Oe in the temperature range 1.8 to 2.4 K (Figure 4) and up to 4 K (Figure S4). The maxima shifted to higher frequencies with increasing temperature, moving out of the frequency limit of the instrument at temperatures above 2.4 K. The quantitative relaxation times, τ, were found by fitting the Cole-Cole plots (χ_M" vs χ_M') for each temperature with the generalized Debye model (solid lines) (Figure 5, left). From the temperature dependence of τ, the barrier height U_{eff} can be determined from the Arrhenius plot of lnτ vs. 1/T (Figure 5, right). The linear portion of the Arrhenius plot is indicative of an Orbach relaxation mechanism,[5i] with a calculated thermal relaxation barrier of U_{eff} = 12.6 cm^{-1} (18.1 K) and a pre-exponential factor of $\tau_0 = 9.3 \times 10^{-8}$. The obtained value of U_{eff} falls into the lower end of values determined for other mononuclear Dy^{3+} complexes.[5e,5g] The non-linear dependence at low temperatures of the Arrhenius plot is indicative of the presence of other relaxation pathways such as Raman and quantum tunnelling processes.[5i,28]

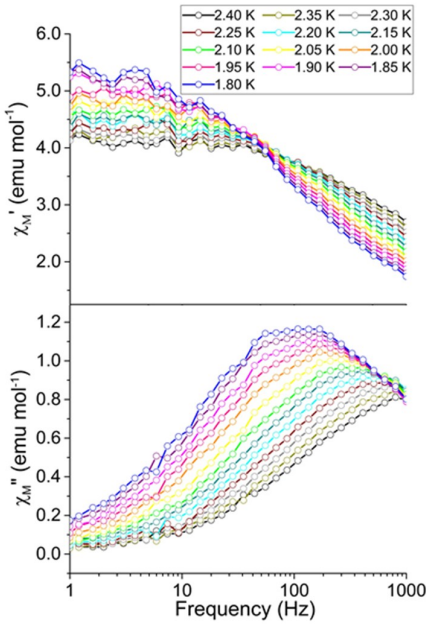

Figure 4. Frequency dependence as a function of the in-phase (χ_M') (top) and out-of-phase (χ_M") (bottom) ac susceptibility measurements of a 12:1 (Y:Dy) magnetic dilution of **1·thf** under a 400 Oe applied dc field and a 2 Oe switching field. Lines are a guide for the eye.

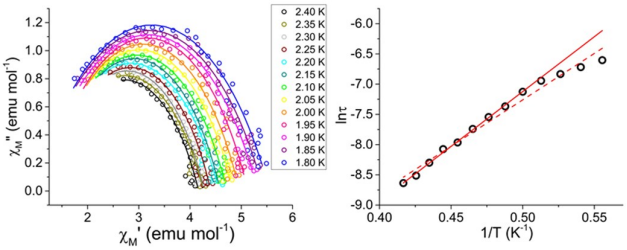

Figure 5. Left: Cole-Cole (Argand) plots for ac susceptibility collected under an applied field of 400 Oe for the 12:1 (Y:Dy) magnetic dilution of **1·thf**, open circles represent experimental data, solid lines represent fits. Right: Arrhenius plot of the 12:1 (Y:Dy) magnetic dilution of **1·thf**. Relaxation times, τ, were determined from non-linear least squares fits to the Cole-Cole plots. Open black circles correspond to experimental data, solid red line corresponds to a fit of the linear portion of the data (T = 2-2.4 K) and dashed red line to a fit of all the data (T = 1.8-2.4 K) to the Arrhenius expression $\tau=\tau_0 exp(U_{eff}/k_BT)$, affording U_{eff} = 12.6 cm^{-1} (18.1 K) and 10.7 cm^{-1} (15.4 K) respectively.

Finally, we were interested in calculating the orientation of the easy axis of the magnetization of the Dy^{3+} ion in **1**. For this purpose, we utilized the quantitative electrostatic model described by Chilton et al. (Figure 6) which uses point charges on the ligand donor atoms.[29] While the anionic charge in an isolated $[CpW(CO)_3]^-$ anion is symmetrically delocalized, the differences in geometric parameters between bridging and end-on carbonyl ligands (see

above) strongly suggest that anionic charge is (at least partially) localized on the bridging carbonyl ligands in **1**.

We considered two different scenarios: First, assuming equivalent binding and charge localization of the three $[CpW(CO)_3]^-$ moieties to Dy^{3+} we calculated the magnetic easy axis shown in orange in Figure 6, which is insensitive to the magnitude of the anionic charge employed for the calculation. Notably, the anionic charges of the isocarbonyl-O atoms apparently enforce the ground state electron density of Dy to be distributed perpendicular to the Dy-isocarbonyl plane. Accordingly, the easy axis is calculated to lie within that very plane.[30]

However, given that the Dy-O1 bond length is roughly 0.05 Å longer than the Dy-O2 and Dy-O3 distances, we also calculated the magnetic easy axis for the Dy^{3+} ion assuming less negative charge on O1 (-0.5) than on O2 (-1) and O3 (-1) (blue axis in Figure 6). The change in orientation is as expected from an electrostatic model.

Overall, we prefer a formulation of equal charge distribution for O1, O2, and O3 (orange line) in **1**.

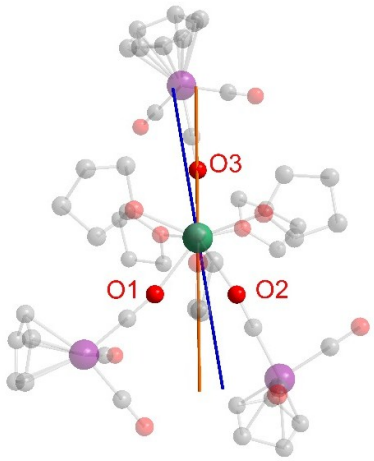

Figure 6. Calculated magnetic anisotropy axes in **1** assuming equivalent negative charges on O1-O3 (orange line) and inequivalent charges for O1 (-0.5), O2 (-1), and O3 (-1) (blue line). The electrostatic calculations were carried out using the FORTRAN program MAGELLAN, developed by Chilton *et al.*[29]

Conclusions

The first structurally characterized dysprosium isocarbonyl complex, $[\{CpW(CO)_2(\mu\text{-}CO)\}_3Dy(thf)_5]$ **1**, has been synthesized from the amine elimination reaction between $[Dy(N(SiMe_3)_2)_3]$ and $[HW(CO)_3Cp]$. Slow magnetic relaxation is observed in a dilute sample of **1·thf** (Y:Dy 12:1) under a 400 Oe applied dc field, with a barrier height (U_{eff}) of 12.6 cm^{-1} (18.1 K). The utilization of lanthanide complexes stabilized by metal-carbonyl fragments may lead to new classes of heterometallic SMMs. Investigations of the electrochemical and photochemical properties of compounds such as **1** are currently ongoing and may allow for the generation of species that feature exchange coupling between lanthanide and paramagnetic transition metal ions through carbonyl bridges.

Acknowledgements

MN is grateful to the TAMU Chemistry Department for generous start-up funds. We thank Toby Woods and Dr. Joseph Zadrozny for helpful discussions.

Notes and references

1 D. Gatteschi, R. Sessoli and J. Villain, *Molecular Nanomagnets*. Oxford University Press, 2006.

2 R. Sessoli, T. H. Lien, A. R. Schake, S. Wang, J. B. Vincent, K. Folting, D. Gatteschi, G. Cristou and D. N. Hendrickson, *J. Am. Chem. Soc.*, 1993, **115**, 1805-1816.; R. Sessoli, D. Gatteschi, A. Caneschi, M. A. Novak, *Nature*, 1993, **365**, 141-143.

3 S. Gómez-Coca, D. Aravena, R. Morales and E. Ruiz, *Coord. Chem. Rev.*, 2015, **289-290**, 379-392.; G. A. Craig and M. Murrie, *Chem. Soc. Rev.*, 2015, **44**, 2135-2147.

4 R. Bagai and G. Christou, *Chem. Soc. Rev.*, 2009, **38**, 1011-1026.; G. Christou, *Polyhedron*, 2005, **24**, 2065-2075.

5 Ln SMMs Reviews: (a) R. Sessoli and A. K. Powell, *Coord. Chem. Rev.*, 2009, **253**, 2328-2341.; (b) L. Sorace, C. Benelli and D. Gatteschi, *Chem. Soc. Rev.*, 2011, **40**, 3092-3104.; (c) J. D. Rinehart and J. R. Long, *Chem. Sci*., 2011, **2**, 2078-2085.; (d) J. Luzon and R. Sessoli, *Dalton Trans*., 2012, **41**, 13556-13567.; (e) D. N. Woodruff, R. E. P. Winpenny and R. A. Layfield, *Chem. Rev.* **2013**, 113, 5110-5148.; (f) P. Zhang, Y.-N. Guo and J. Tang, *Coord. Chem. Rev.*, 2013, **257**, 1728-1763.; (g) H. L. C. Feltham and S. Brooker, *Coord. Chem. Rev.* 2014, **276**, 1-33.; (h) K. Lui, W. Shi and P. Cheng, *Coord. Chem. Rev.* 2015, **289-290**, 74-122.; (i) S. T. Liddle and J. van Slageren, *Chem. Soc. Rev.*, 2015, **44**, 6655-6669.; (j) R. A. Layfield and M. Murugesu, *Lanthanides and Actinides in Molecular Magnetism*. Wiley-VCH: Weinham, 2015.; (k) C. Benelli and D. Gatteschi, *Introduction to Molecular Magnetism : From Transition Metals to Lanthanides*. Wiley-VCH: Weinham, 2015.; (l) J. Dreiser, *J. Phys.: Condens. Matter*, 2015, **27**, 183203.

6 N. Ishikawa, M. Sugita, T. Ishikawa, S.-y. Koshihara and Y. Kaizu, *J. Am. Chem. Soc.*, 2003, **125**, 8694-8695.

7 C. R. Ganivet, B. Ballesteros, G. de la Torre, J. M. Clemente-Juan, E. Coronado and T. Torres., *Chem.-Eur, J*., 2013, **19**, 1457-1465.

8 R. J. Blagg, L. Ungur, F. Tuna, J. Speak, P. Comar, D. Collison, W. Wernsdorfer, E. J. L. McInnes, L. F. Chibotaru and R. E. P. Winpenny, *Nat. Chem.*, 2013, **5**, 673-678.

9 S. Demir, I.-R. Jeon, J. R. Long and T. D. Harris, *Coord. Chem. Rev.*, 2015, **289-290**, 149-176.; J. D. Rinehart, M. Fang, W. J. Evans and J. R. Long, *J. Am. Chem. Soc.*, 2011, **133**, 14236-14239.

10 L. R. Piquer and E. C. Sañudo, *Dalton Trans.*, 2015, **44**, 8771-8780.

11 (a) L. Ungur, J. J. Le Roy, I. Korobkov, M. Murugesu and L. F. Chibotaru, *Angew. Chem. Int. Ed*., 2014, **53**, 4413-4417.; (b) T. Pugh, F. Tuna, L. Ungur, D. Collison, E. J. L. McInnes, L. F. Chibotaru and R. A. Layfield, *Nat. Commun.*, 2015, **6**, 7492.

12 I. P. Beletskaya, A. Z. Voskoboynikov, E. B. Chuklanova, N. I. Kirillova, A. K. Shestakova, I. N. Parshina, A. I. Gusev and G. K.-I. Magomedov, *J. Am. Chem. Soc*., 1993, **115**, 3156-3166.; B. E. Bursten and M. G. Gatter, *J. Am. Chem. Soc*., 1984, **106**, 2554-2558.

13 C. A. Ghilardi, S. Mindollini and L. Sacconi, *J. Organomet. Chem.*, 1980, **186**, 279-287.

14 J. H. Osborne, A. L. Rheingold and W. C. Trogler. *J. Am. Chem. Soc.*, 1985, **107**, 6292-6297.

15 A. L. Ward, W. W. Lukens, C. C. Lu and J. Arnold, *J. Am. Chem. Soc.*, 2014, **136**, 3647-3654.

16 For examples of other lanthanide isocarbonyl compounds see Yb: (a) T.D. Tilley and R. A. Anderson, *J. Am. Chem. Soc.*, 1982, **104**, 1772-1774.; (b) M.P. Blake, N, Kaltsoyannis and P. Mountford, *Chem. Commun.*, 2013, **49**, 3315-3317.; (c) M.P. Blake, N. Kaltsoyannis, P. Mountford, *J. Am. Chem. Soc.*, 2011, **133**, 15358-15361.; (d) C. Doring, A.-M. Dietel, M.V. Butovskii, V. Bezugly, F. R. Wagner, R. Kempe, *Chem.-Eur. J.*, 2010, **16**, 10679-10683.; (e) (and Sm) S. N. Konchenko, T. Sanden, N. A. Pushkarevsky, R. Koppe, P. W. Roesky, *Chem.-Eur. J.*, 2010, **16**, 14278-14280.; (f) J. M. Boncella and R. A. Anderson, *Inorg. Chem.*, 1984, **23**, 432-437.; (g) P. V. Poplaukhin, X. Chen, E. A. Meyers and S. G. Shore, *Inorg. Chem.*, 2006, **45**, 10115-10125.; (h) (and Sm) A. C. Hiller, A. Sella and M. R. J. Elsegood, *J. Chem. Soc., Dalton Trans.*, 1998, 3871-3874.; (i) Z. Hou, K. Aida, Y. Takagi and Y. Wakatsuki, *J. Organomet. Chem.*, 1994, **473**, 101-104.; (j) C.E. Plecnik, S. Liu, J. Liu, X. Chen, E. A. Meyers and S. G. Shore, *Inorg. Chem.*, 2002, **41**, 4936-4943.; (k) K. Muller-Buschbaum, G.B. Deacon and C.M. Forsyth, *Eur. J. Inorg. Chem.*, 2002, 3172-3177. La: (l) A. A. Pasynskii, I. L. Eremenko, G. Z. Suleimanov, Y. A. Nuriev, I. P. Beletskaya, V. E. Shklover and Y. T. Struchkov, *J. Organomet. Chem.*, 1984, **266**, 45-52.; Sm (m) G. Li and W.-T. Wong, *J. Organomet. Chem.*, 1996, **522**, 271-275.; (n) A. C. Hillier, S. Y. Liu, A. Sella, O. Zekria and M. R. J. Elsegood, *J. Organomet. Chem.*, 1997, **528**, 209-215.; (o) A. Recknagel, A. Steiner, S. Brooker, D. Stalke and F.T. Edelmann, *Chem. Ber.*, 1991, **124**, 1373-1375.; Eu: (p) C.E. Plecnik, S. Liu, X. Chen, E. A. Meyers and S. G. Shore, *J. Am. Chem. Soc.*, 2004, **126**, 204-213.; Ce: (q) P. N. Hazin, J. C. Huffman and J. W. Bruno, *Chem. Commun.*, 1988, 1473-1474.
17 D. C. Bradley, J. S. Ghotra and F. A. Hart, *J. Chem. Soc., Dalton Trans.*, 1973, 1021-1023.; P. Zheng, L. Zhang, C. Wang, S. Xue, S.-Y. Lin and J. Tang, *J. Am. Chem. Soc.*, 2014, **136**, 4484-4487.
18 A. P. Sobaczynski, J. Obenauf and R. Kempe. *Eur. J. Inorg. Chem.* 2014, 1211-1217.
19 SAINT and APEX 2 Software for CCD Diffractometers, Bruker AXS Inc., Madison, WI, USA, 2014.
20 G. M. Sheldrick, SADABS, version 2.03, Bruker Analytical X-ray Systems, Inc., Madison, WI, 2000.
21 (a) G. M. Sheldrick, Acta. Cryst. Sect. A, 2007, 64, 112-122.; (b) G. M. Sheldrick. SHELXT, University of Göttingen, Germany, 2014.; (c) G. M. Sheldrick. SHELXL, University of Göttingen, Germany, 2014.; (d) O. V. Dolomanov, L. J. Bourhis, R. J. Gildea, J. A. K. Howard and H. Puschmann, *J. Appl. Crystallogr.*, 2009, **42**, 339-341. (e) OLEX2: a complete structure solution, refinement and analysis program O. V. Dolomanov, L. J. Bourhis, R. J. Gildea, J. A. K. Howard and H. Puschmann, *J. Appl. Cryst.*, 2009, **42**, 339-341.
22 G. A. Bain and J. F. Berry, *J. Chem. Educ.*, 2008, **85**, 532-536.
23 (a) A. E. Crease and P. Legzdins, *J. Chem. Soc., Dalton Trans.*, 1973, 1501-1507.; (b) G. Z. Suleimanov, L. F. Rybakova, A. B. Sigalov, Y. A. Nuriev, N. S. Kochetkova, I. P. Beletskaya, *Zh. Org. Khim.*, 1982, **18**, 2482-2485.; (c) G. Z. Suleimanov, I. P. Beletskaya, *Dokl. Akad. Nauk*, 1981, **261**, 381-383.; (d) X. Wang, X. Zhou, Y. Wang, *Guangpuxue Yu Guangpu Fenxi*, 1987, 7, 28-30.; (e) X. Wang, X. Zhou, J. Zhang, Y. Xia, R. Lui, S. Wang, *Kexue Tongbao (Foreign Language Edition)*, 1985, **30**, 351-355. (f) S. Li, X. Yang, Y. Sun, P. Li, X. Wang and X. Zhou, *Gaodeng Xuexiao Huaxue Xuebao*, 1988, **9**, 1242-1245. (g) P.-F. Yan, J.-S. Gao, Z.-Y. Le, G.-J. Mao, *Gaodeng Xuexiao Huaxue Xuebao*, 1998, **19**, 21-23.
24 M. Y. Darensbourg and H. L. C. Barros, *Inorg. Chem.* 1979, **18**, 3286-3288.; M. Y. Darensbourg and J. M. Hanckel, *Organometallics*, 1982, **1**, 82-87.
25 S.-D. Jiang, B.-W. Wang, G. Su, Z.-M. Wang and S. Gao, *Angew. Chem. Int. Ed.* 2010, **49**, 7448.
26 Y. Bi, Y.-N. Guo, L. Zhao, Y. Guo, S.-Y. Lin, S.-D. Jiang, J. Tang, B.-W. Wang and S. Gao, *Chem.-Eur. J.*, 2011, **17**, 12476.
27 D. Gatteschi and R. Sessoli, *Angew. Chem. Int. Ed.*, 2003, **42**, 268-297.
28 S. Demir, J. M. Zadrozny and J. R. Long, *Chem.-Eur. J.*, 2014, **20**, 9524-9529 and references therein.
29 N. F. Chilton, D. Collison, E. J. L. McInnes, R. E. P. Winpenny and A. Soncini, *Nat. Commun.*, 2013, **4**, 2551.
30 S.-S. Liu, X. Ling, S.-D. Jiang, Y.-Q. Zhang, Y.-S. Meng, Z. Wang, B.-W. Wang, W.-X. Zhang, Z. Xi and S. Gao, *Inorg. Chem.*, 2015, **54**, 5162-5168.